A multiresponsive functional AIEgen for spatiotemporal pattern control and all-round information encryption

Xinyuan He,[1] Jianyu Zhang,[1] Xinyue Liu,[1] Zhuwei Jin,[1] Jacky W. Y. Lam,[1,*] and Ben Zhong Tang[1,2,3,*]

[1] Department of Chemistry, Hong Kong Branch of Chinese National Engineering Research Center for Tissue Restoration and Reconstruction, and Guangdong-Hongkong-Macou Joint Laboratory of Optoelectronic and Magnetic Functional Materials, The Hong Kong University of Science and Technology, Clear Water Bay, Kowloon, Hong Kong, China

[2] Center for Aggregation-Induced Emission, South China University of Technology, Guangzhou, 510640, China

[3] School of Science and Engineering, Shenzhen Institute of Aggregate Science and Technology, The Chinese University of Hong Kong, Shenzhen, Guangdong, 518172, China

Correspondence and requests for materials should be addressed to J.W.Y.L or B.Z.T. (e-mail: chjacky@ust.hk or tangbenz@cuhk.edu.cn)

Keywords: multiresponses, aggregation-induced emission, primary amines, photoarrangement, information encryption

Abstract: Functional materials with multi-responsive properties and good controllability are highly desired for developing bioinspired and intelligent multifunctional systems. Although some chromic molecules have been developed, it is

still challenging to realize in-situ multicolor fluorescence changes based on a single luminogen. Herein, we reported an aggregation-induced emission (AIE) luminogen called CPVCM, which can undergo a specific amination with primary amines to trigger luminescence change and photoarrangement under UV irradiation at the same active site. Detailed mechanistic insights were carried out to illustrate the reactivity and reaction pathways. Accordingly, multiple-colored images, a quick response code with dynamic colors, and an all-round information encryption system were demonstrated to show the properties of multiple controls and responses. It is believed that this work not only provides a strategy to develop multiresponsive luminogens but also develops an information encryption system based on luminescent materials.

Introduction

Creatures exhibit remarkable wisdom in coloration.[1,2] Numerous animals have evolved adaptive coloration in response to the living environment, which involves a striking array of color strategies feasible in defending against natural enemies.[3-5] However, some intelligent animals prefer to perform dynamic coloration and better serve multiple and sometimes conflicting functions. For example, chameleons and cuttlefishes change their external appearance timely to hide from predators.[6-9] Orchid mantises take the guise of a whole flower blossom for hunting and attract pollinators as prey even far from flowers.[10] Crested ibis put on nuptial plumage coloration in the mating season to maximize detectability to conspecifics and boosts the reproductive success of individuals.[11] Such excellent examples in nature provide continuous inspiration for

scientists.

Intelligent systems with multifunctions are one long-lasting desire. One promising approach is to use stimuli-responsive luminogens to mimic the dynamic coloration of animals.[12-14] Although numerous "smart" luminogens have been developed recently, a rough "adaptive coloration" is achieved in most cases because the reported luminogens are monoresponsive.[15-19] Even when a complex combination of luminogens is further applied, the obtained multi-colored images are usually traceable.[20-23] On the other hand, the current reported multiresponsive luminogens often lack good controllability.[24-27] For instance, Xu et al. reported one luminogens that showed multi-emission in respond to pH change, but the sensitivity and spatial resolution were low.[24] Jiang et al. developed spiropyran derivatives with solid photochromism and mechanochromism but failed to operate grinding in the artificial template.[25] As a result, novel multi-responsive luminogens with more than one easy-operated control are desired for both simplification and security. Besides, multi-model control is expected to make artificial systems alive. By utilizing synthetic organic chemistry, at least three desirable coloration models were built, which exhibited: (i) reproducible coloration produced by reversible reactions,[28] (ii) remote or noncontact coloration enabled from photo-reactions,[29-31] or (iii) time-dependent coloration based on spontaneous chemical reactions.[32,33] However, it is challenging to meet good controllability in these models based on a single luminogen. Moreover, luminogens should undergo robust discoloration in the solid state to achieve the solvent-free system and pursue applications as solid devices. Conceivably, if one molecule meets all these requirements,

its limitless applications are expected.

The phenomenon of aggregation-induced emission (AIE) was first coined by Prof. Tang in 2001,[34] which refered to a class of luminogens that showed intensified emission in the aggregate state.[35,36] Because of this unique property, luminogens with AIE effect (AIEgens) are promising for solid-state luminescence. Previously, we reported an AIEgen called CMVMN which could undergo specific bioconjugation with primary amines and a rapid and spontaneous reversible amination process in its electrospun films.[37] In view of the great potential of this amination process for developing functional systems, a further study on its mechanism is definitely of academic importance. Coincidently, a concise and efficient photoarrangement was observed for the arylvinyl-substituted chromones.[38] Thus, we are wonder whether it is possible to obtain a hybrid compound that is capable of undergoing both spontaneously reversible amination and photochromism so that we can further investigate these two processes and pursue multiresponsive applications.

In this work, we designed and synthesized an AIEgen, namely (*Z*)-2-{5,5-dimethyl-3-[2-(4-oxo-4H-chromen-3-yl)-1-phenylvinyl]cyclohex-2-en-1-ylidene}malononitrile and abbreviated as CPVCM (Fig. 1) that could undergo both an amination with primary amines and photoarrangement with self-reporting property. The amination was fast, reversible and highly specific, and gave a distinct color change and red-shifted fluorescence. Meanwhile, a sensitive photoarrangement accompanied with blue-shifted emission was observed. NMR titration and theoretical calculation were further conducted to study the mechanisms of the two processes. By utilizing this

multiresponsive and multicontrollable molecule, dip-coated films were fabricated to realize colored images and dynamic quick response (QR) codes, and a multicolor and all-round information encryption system was further built. Thus this work not only developed a novel AIE skeleton with multiple responses and controls but also provided a strategy for dynamic information encryption based on luminescent materials.

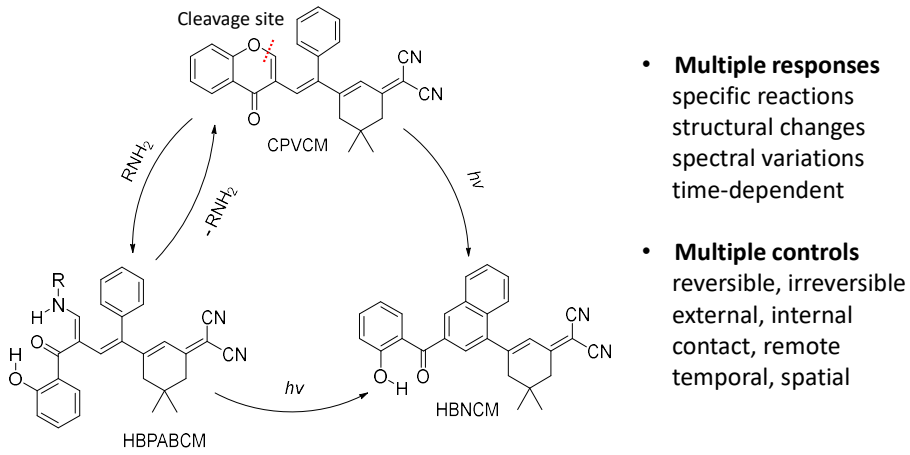

Fig. 1 Design strategy of molecule with multiple responses and controls. Specific amination with primary amines and photoarrangement of CPVCM.

Results and Discussion

Photophysical Properties. CPVCM was synthesized according to the synthetic route shown in Supplementary Fig. 1. The intermediate and the final product were characterized spectroscopically and satisfactory results corresponding to their molecular structures were obtained (Supplementary Fig. 2-7). The photophysical properties of CPVCM were firstly investigated. CPVCM absorbed at 390 nm (Supplementary Fig. 8) and emitted weakly at 510 nm (Fig. 2a) in tetrahydrofuran (THF) solution. When a poor solvent of water was added to the THF solution, gradually enhanced fluorescence was observed owing to the aggregate formation. At a water

fraction (f_w) of 99%, the fluorescence intensity was 8-fold higher than that in pure THF solution (f_w = 0%), which verified its AIE property.

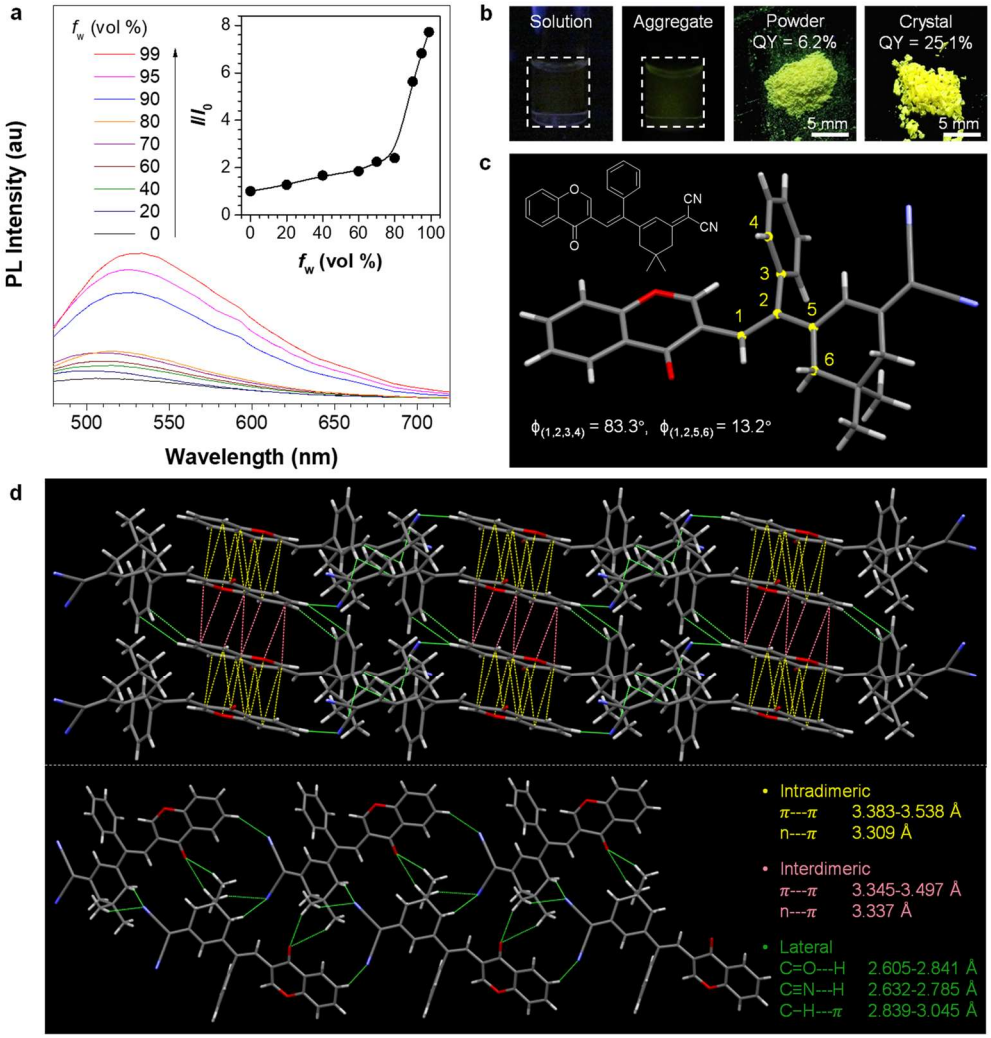

Fig. 2 Photophysical property and single-crystal structure. (a) Photoluminescence (PL) spectra of CPVCM (10 μM) in THF/water mixtures with different water fractions (f_w). Inset: Plots of I/I_0 value versus the f_w of THF/water mixtures of CPVCM, where I_0 = PL intensity in pure THF solution. λ_{ex} = 390 nm. (b) Photographs of CPVCM in solution (f_w = 0%) and aggregate suspension in THF/water mixtures (f_w = 99%), and its amorphous powder and crystalline solid taken under UV illumination. Scale bar: 5 mm. (c) Crystal structure of CPVCM. Inset: Chemical structure of CPVCM and the dihedral angles in the crystal structure. (d) Crystal packing of CPVCM molecules with multiple intermolecular interactions.

Although CPVCM showed very weak emission in the aggregate suspension, its powder and solid crystals were highly emissive with a quantum yield (QY) of 6.2% and 25.1%, respectively (Fig. 2b and Supplementary Fig. 9). Such a phenomenon was also observed in many reported AIEgens and is termed as crystallization-induced emission.[39,40] On the other hand, the films of CPVCM fabricated by spin-coating of its dichloromethane was also emissive though as not as strong of that of powder and solid crystals. The XRD diffractograms of the spin-coated film exhibited no sharp peak but a diffuse halo at high angle, demonstrating its non-crystalline nature (Supplementary Fig. 9). It also suggested that CPVCM might easily crystalize to form nanocrystals with reasonable emission in the powder state.

Single-crystal X-ray diffraction technique was then utilized to investigate the crystal structure and intermolecular interactions of CPVCM. As shown in Fig. 2c and Supplementary Table 1, the dihedral angle between the two double bonds ($\phi_{(1,2,5,6)}$) was 13.2°and the benzene ring was almost perpendicular to the double bond ($\phi_{(1,2,3,4)}$ = 83.3°). These indicated that CPVCM adopted a twist conformation. In the crystal state, the molecules of CPVCM exhibited face-to-face patterns of chromone moieties and formed a dimeric structure (Fig. 2d). Besides, numerous strong intramolecular interactions, including intradimeric, interdimeric and lateral interactions were observed, which helped rigidity the molecular conformation to result in intensified emission in the crystalline state.[41,42] On the other hand, abundant intradimeric interactions were observed only between two chromone rings, which mainly affected the molecular motion of the chromone rings. Therefore, even dimers might be formed in aggregates

suspension in poor solvent or in spin-coating films, the molecular packing was so loose that might enable the molecues to undergo molecular motions to give rise to weak emission. The above results illustrated the photophysical properties of CPVCM and might also offer it a new coloration model.

Amination with primary amines. To test the reactivity of CPVCM to primary amines, propylamine (PA) was chosen as the model amine and was added to a solution of CPVCM. As shown in Fig. 3a, the typical absorption peak of CPVCM at 390 nm disappeared and was replaced by a new peak at 475 nm, which favored the direct visualization of the amination process. Meanwhile, a turn-on fluorescence signal at 585 nm was detected, and the intensity increased by 77 times at a PA concentration of 10 mM. Besides, the amination process proceeded rapidly, and the fluorescence intensity reached its maximum and a plateau within 4 min (Fig. 3b). Therefore, the above results supported that CPVCM could serve as a fluorescent and colorimetric dual-mode probe for sensitive detection of PA.

Then, the fluorescence response of CPVCM to various amines, including primary amines, secondary amines, tertiary amines, aromatic amines, and ammonia, was investigated (Fig. 3c). As expected, dramatic fluorescence enhancement was only observed for aliphatic primary amines. Based on the experimental data and our previous report[37], a schematic illustration of the selectivity of CPVCM to amines was proposed in Fig. 3d. The nucleophilicity of amines is an essential factor to determine their reactivity. The alkyl units were generally regarded as electron-donating groups because the electrons around the α carbon were drawn to the nitrogen atom. Still, the inductive

donating effect was diminished with distance. Interestingly, the fluorescence signal increased with the length of the alkyl chain (amylamine > butylamine > PA), which indicated that the amination process proceeded better with amines of high nucleophilicity. For benzylamine, the through-space n···π conjugation partially reduced its nucleophilicity to resulted in weak reactivity and fluorescence.[43,44] For aniline and ammonia, almost no fluorescence enhancement was observed since their nucleophilicity was greatly reduced by the strong through-bond n···π conjugation[45,46] and the hydration[47], respectively.

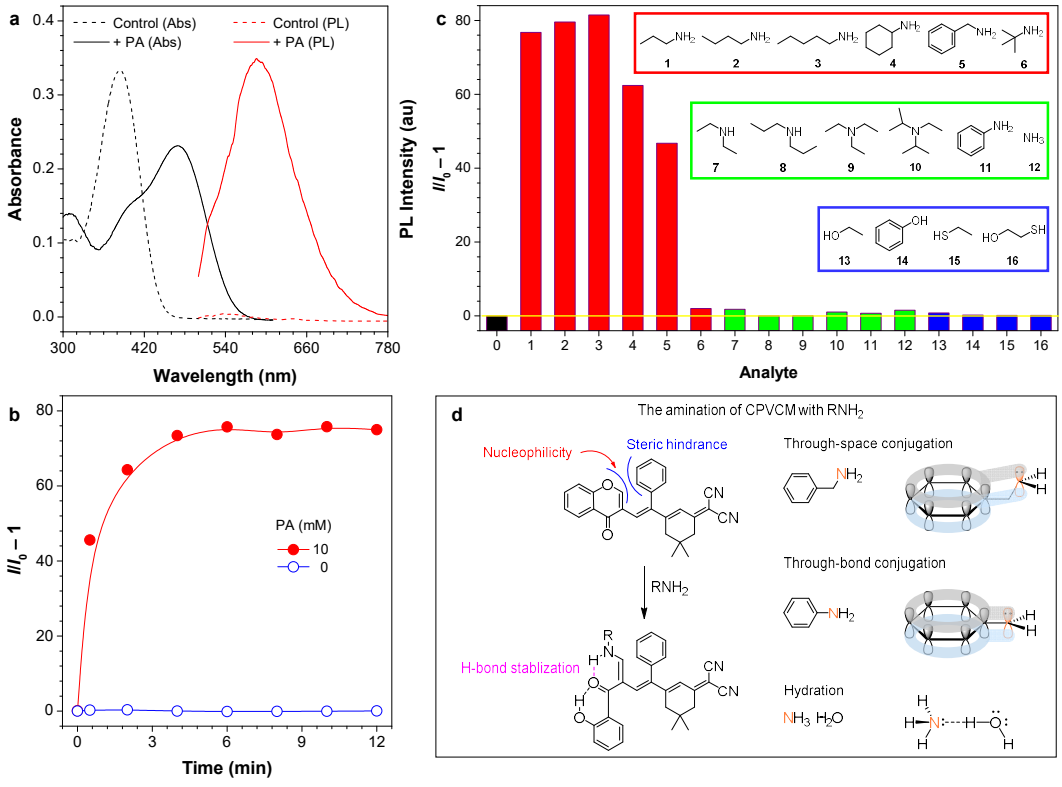

Fig. 3 Reaction between CPVCM and nucleophiles. (a) Absorption and photoluminescence (PL) spectra of CPVCM (10 μM) before (control) and after reaction with PA (10 mM) in THF. (b) Time course of the amination reaction of CPVCM (10 μM) with PA. (c) Relative fluorescence intensity ($I/I_0 - 1$) of CPVCM (10 μM) after mixing with different analytes (10 mM). Analyte: [(0) CPVCM (control)], (1) PA, (2) butylamine, (3) amylamine, (4) cyclohexylamine, (5) benzylamine, (6) *tert*-butylamine, (7) diethylamine, (8) dipropylamine, (9) trimethylamine, (10) *N,N*-

diisopropylethylamine, (11) aniline, (12) ammonia, (13) ethanol, (14) phenol, (15) ethanethiol, (16) mercaptoethanol. Inset: chemical structures of the analytes investigated in this study. $\lambda_{ex/em}$ = 475/585 nm. (d) Schematic illustration of the reaction between CPVCM and nucleophiles.

Except for nucleophilicity, steric hindrance also affected the amination process. A noticeable decrease in fluorescence intensity was observed by increasing the steric hindrance of the molecules (tert-butylamine > benzylamine > cyclohexylamine). Compared with CMVMN in our previous work,[37] CPVCM was introduced with an additional phenyl group. Therefore, the amination of CPVCM was expected to be more sensitive to the steric hindrance of amines. Indeed, the obtained results were in accordance with our expectation: the amination process was slow down with an increase of the steric effect of amines and almost no fluorescence response was detected when steric *tert*-butylamine was used as nucleophile (Fig. 3b).

Additionally, hydrogen-bond stabilization is tightly associated with the selective amination of CPVCM with primary amines as it can stabilize the product and facilitate the forward reaction. The hydrogen bond (N-H···O) only existed in the amination products of CPVCM and primary amines. Combined with the high steric hindrance of secondary amines and tertiary amines, it is reasonable that no obvious fluorescence enhancement was observed. Notably, the electronegativity of chalcogens like sulfur (2.58) and oxygen (3.44) was similar to that of nitrogen (3.04), and the electronegativity and the strength of a nucleophile usually showed an inverse relationship. Therefore, at least alkyl sulfhydrate is comparable to aliphatic primary amines in terms of steric hindrance and nucleophilicity. However, in reality when nucleophiles with hydroxyl or

sulfhydryl group were added, no obvious reaction with CPVCM was observed, which further proved the vital role of the hydrogen-bond stabilization on the amination process. Thus, under the combined effects of nucleophilicity, steric hindrance, and hydrogen-bond stabilization, CPVCM showed high reactivity and selectivity to primary amines.

The reaction of CPVCM with PA was then monitored by ^{1}H NMR and high-resolution mass spectroscopies. As shown in Supplementary Fig. 10, a characteristic broad peak emerged at δ 10.5, which was attributed to the resonance of an NH group forming a strong intermolecular hydrogen bond.[37,48] Also, numerous new peaks appeared at a lower field due to the deshielding effect in the ring-opening products. These results are similar to those of our previous work. Additionally, the mass spectrum showed a mass-to-charge ratio of 500.2308 $[M+Na]^{+}$ associated with the enamine product (Supplementary Fig. 11). Hereby, CPVCM may follow the traditional reaction path of typical chromones. In addition, a reversible amination process was witnessed by adding trifluoroacetic acid (Supplementary Fig. 12). Hopefully, this specific amination process provides new sight into the design of probes and functional systems.

Photoarrangement. Due to the presence of the moiety of arylvinyl substituted chromone, CPVCM is also anticipated to undergo photoarrangement to form its constitutional isomer called HBNCM (Supplementary Fig. 13). To prove this, the chloroform solution of CPVCM was irradiated under a mercury light for 2 h. Afterwards, the solvent was evaporated and the residue was purified by column chromatography and analyzed spectroscopically. As shown in Supplementary Fig. 14-16, satisfactory analysis results according to the molecular structure of HBNCM were

obtained, indicative of the photosensitivity of CPVCM. To follow the reaction, dynamic ^{1}H NMR analysis was conducted by irradiating solution of CPVCM by 365 nm light from a hand-held UV lamp for different time. As depicted in Fig. 4a and Supplementary Fig. 17, a new sharp peak attributed to the resonance of –OH group forming a strong intermolecular hydrogen bond appeared at δ 11.9, whose intensity was intensified with the irradiation time.[48] Also, the intensity of many characteristic peaks at δ 8.2-8.3, 7.1-7.5 and 6.4-6.5 decreased and were replaced by new peaks at δ 7.9-8.2 and 6.9-7.0. The ^{1}H NMR spectrum of CPVCM irradiated by UV light for 1 h was compared with that of HBNCM (Fig. 4a). The similarity in the spectral pattern of the irradiated solution of CPVCM and HBNCM and the appearance of the same peak with a mass-to-charge ratio of 417.1598 in both MS spectra (Supplementary Fig. 18) confidentially supported that CPVCM underwent a photoarrangement and formed solely HBNCM without generating any side products.

The fluorescence response of CPVCM to UV irradiation was also investigated. Upon UV irradiation at 365 nm, a blue-shifted and increased emission peak at around 500 nm was observed, which verified the photochromism of CPVCM (Fig. 4b). The QY increased from 0.6% to 2.2% after 1 min of irradiation, which might be attributed to the better rigidity of HBNCM. Also, the fluorescence intensity almost reached the plateau after 50 s of irradiation, indicative of a fast and traceable photoarrangement process. Besides, a similar absorption blue-shift was observed (Supplementary Fig. 19). Eventually, the absorption spectrum resembled to that of HBNCM (Supplementary Fig. 20), which was consistent with the expected photoarrangement process of CPVCM.

Moreover, HBNCM exhibited aggregation-induced emission and the fluorescence intensity in THF increased gradually upon water addition (Fig. 4c). Combined with the fast photochromic behavior of the spin-coating films of CPVCM under UV irradiation (Supplementary Fig. 21), CPVCM could be capable of conducting fast and UV light-controlled coloration in the solid state.

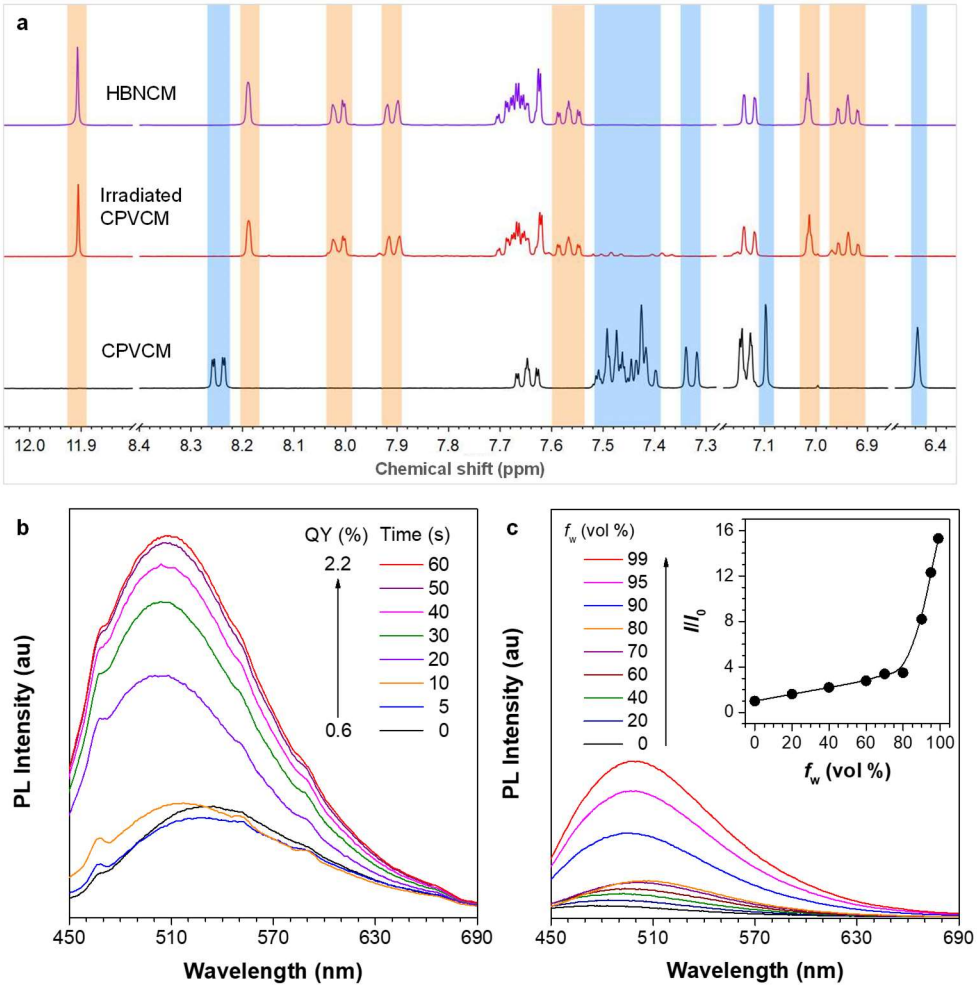

Fig. 4 Photoarrangement of CPVCM and photophysical properties of HBNCM. (a) ^{1}H NMR spectra of CPVCM in $CDCl_3$ before and after irradiation by a 365 nm UV lamp for 1 h. CPVCM was highlighted in blue, while HBNCM was highlighted in orange. (b) Change of PL spectrum of CPVCM (10 μM) in THF/water mixture (f_w = 99%) with irradiation time. λ_{ex} = 350 nm. (c) PL spectra of HBNCM (10 μM) in THF/water mixtures with different water fractions (f_w). Inset: Plot of relative PL intensity I/I_0 versus the composition of the THF/water mixture of HBNCM, where I_0

= PL intensity in pure THF solution. λ_{ex} = 350 nm.

Later, density functional theory calculation was carried out to illustrate the reaction pathway of photoarrangement, and the energy profiles were given in Fig. 5. The UV irradiation of CPVCM led to the formation of an unstable ring-close intermediate called INT1 via a 6π-electron-cyclization. Followed by a [1,9]-H shift, a relatively stable intermediate (INT2) will form with a low energy of −8.00 kcal/mol. The following rearomatization and bond rotation resulted in the generation of the final product, which was stabilized by an intramolecular hydrogen bond and showed stronger emission than CPVCM. Since the energy barriers for the three processes were high, UV irradiation was necessary to excite the molecule to overcome these energy barriers. Considering the specific peaks observed in the ^{1}H NMR spectra in Supplementary Fig. 17 and an abnormal decrease in the fluorescence intensity after 5 s of irradiation (Fig. 4b), it was possible that the metastable and non-emissive INT2 enriched in the early stage. This mechanistic insight of the photoarrangement not only pointed out the reaction pathways of CPVCM but also provided new possibilities for molecular engineering.

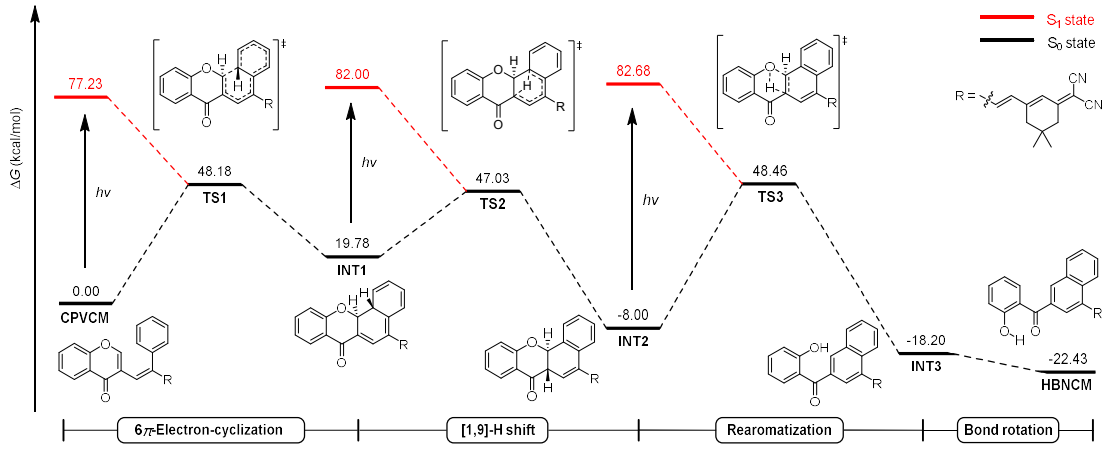

Fig. 5 Proposed mechanism of the photoarrangment of CPVCM. Energy profile for the

photoarrangement of CPVCM.

Spatiotemporal pattern control. Due to the multi-responsive behavior of CPVCM, we further develop it into multifunctional systems. A colorless and non-emissive AIE plate was obtained by dip-coating a thin-layer chromatography (TLC) plate into a DCM solution of CPVCM followed by rapid air-drying process (Fig. 6a and 6b). Then, a "writing" process was conducted through photopatterning with a homemade mask of a "butterfly" image. As a result, a blue-emissive "butterfly" image was clearly displayed in the AIE plate under UV illumination. It is worth noting that although a 365 nm hand-held UV lamp was used as light irradiation source for all investigations, a longer time (1 min) and a shorter distance (5 cm) were required for generating photopattern than for performing fluorescence imaging under UV illumination (1 s; 20 cm). The illumination process caused no damage on the AIE plate, as evidenced by the dark background of the written AIE plate. Later, when the AIE plate was fumed with PA vapor, the surrounding area of the "butterfly" image appeared orange and red under daylight and UV illumination, respectively. Thus, CPVCM itself was capable of *in-situ* fabricating multicolor images.

The amination and photoarrangement of CPVCM occurred at the same position of the chromone ring. As a result, these two processes cannot occur simultaneously but could be manipulated according to the sequence of the two processes. Accordingly, the two areas of the well-defined multicolor "butterfly" button showed different coloration after PA fuming, suggesting the controllable coloration of CPVCM. Besides, the amination was reversible but the photoarrangement was irreversible, which made the

UV irradiation a method of higher priority than the PA fuming in the discoloration of CPVCM. As expected, when the written AIE plate was directly irradiated by UV light, the whole pattern became blue-emissive, and no "butterfly" could be observed anymore in the erased AIE template (Fig. 6b). In a word, controllable writing and erasing processes were realized by solely a single molecule of CPVCM.

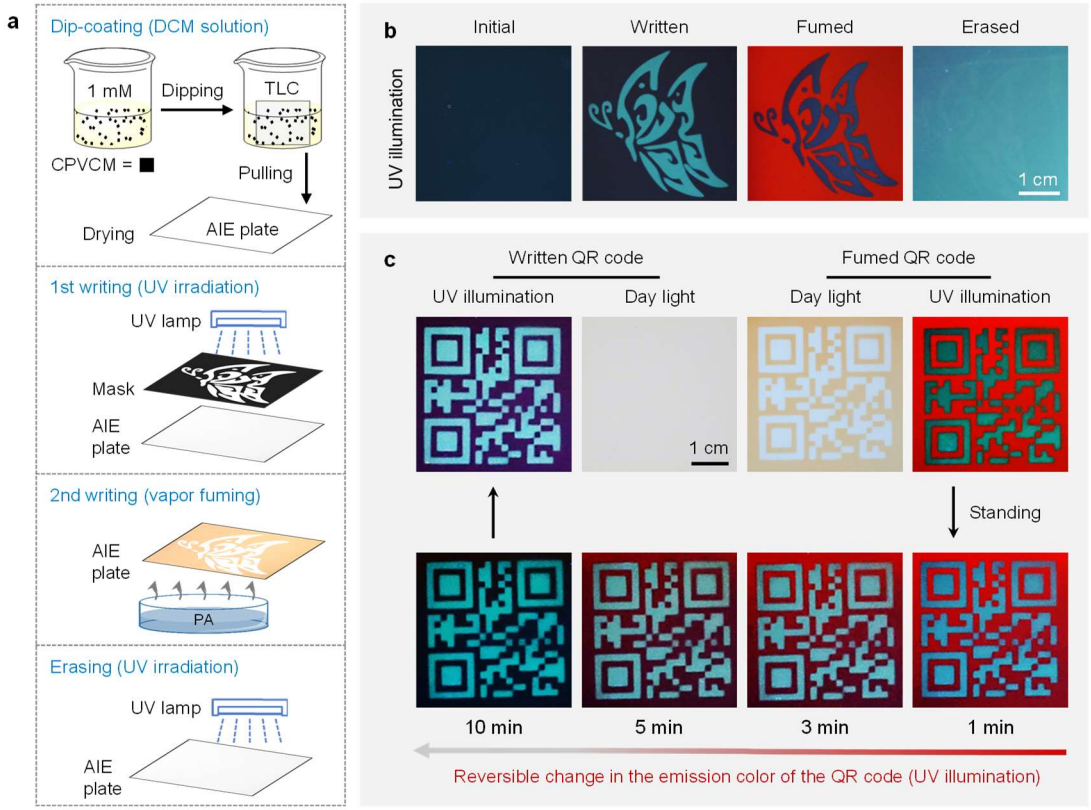

Fig. 6 Applications in developing multiple-colored images and quick response code. (a) Schematic illustration of the dip-coating of CPVCM (1 mM in DCM) on a TLC plate and the corresponding writing processes through UV irradiation (1 min) and fuming (PA for 10 s) and further erasing process. (b) Fluorescent images of the developed multicolor "butterfly" pattern. (c) Photographs of the developed colored "QR code" and the time course of reversible changes in the emission color of the "QR code".

Dynamic coloration, on the other hand, is particularly interesting for applications like information encryption and 4D printing.[21-23,33] Because of the reversible amination

process of CPVCM, a written quick response (QR) code was further manufactured through photopatterning on an initial AIE plate. Similarly, the written QR code could only be read under UV illumination, while the fumed QR code became orange and emitted both blue and red fluorescence under daylight and UV illumination, respectively (Fig. 6c). But if the fumed plate was put in the open air, the red-emissive area gradually faded and disappeared in 10 mins. A reversible color change was also observed in the daylight (Supplementary Fig. 22), demonstrating the great potential of CPVCM for dynamic coloration.

All-round information encryption: The versatile properties and multiple responses of CPVCM inspire us to explore its practical applications. While the amination process worked in the contact model, the photoarrangment enabled remote control. One possibility was to unilaterally hinder the amination process by using a transparent thermoplastic such as polymethyl methacrylate (PMMA). Subsequently, a DCM solution of CPVCM (1 mM) containing different concentrations of PMMA was chosen as the security ink to fabricate a sensor with an elephant image on a filter paper by painting (Fig. 7a). For CPVCM alone, the initial image was olive-emissive and similar to that of CPVCM powder possibly due to the formation of nanocrystals. While the emission color turned red after PA fuming, the expected blue emission was not observed for the irradiated sensor. The strongly rigidified structure of CPVCM in the nanocrystals possibly had hindered the photoarrangement process. Thus, the fluorescence signal mainly came from the nanocrystals.

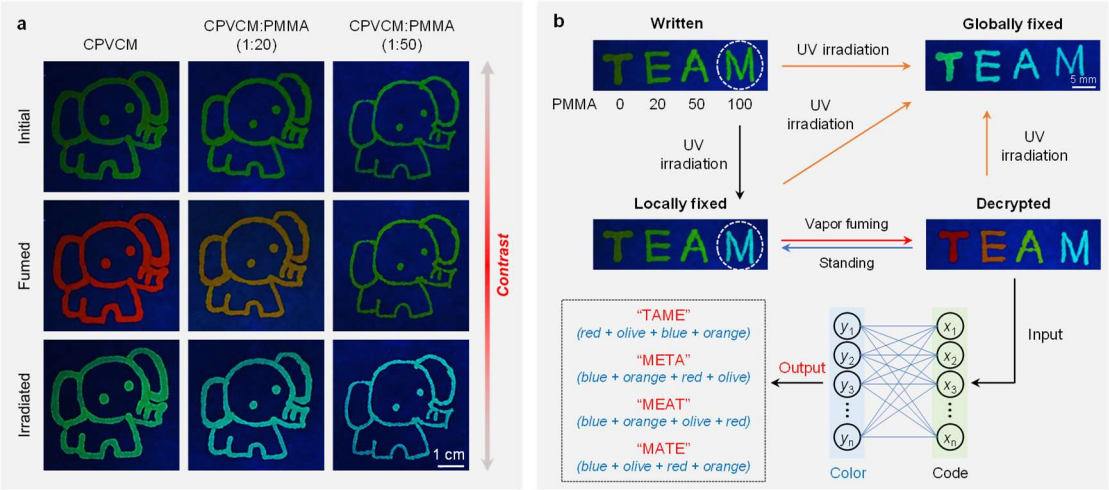

Fig. 7 Applications in all-round information encryption. (a) Fluorescent images of the initial sensors with an "elephant" image painted from the CPVCM (1 mM) security ink with different concentrations of PMMA (0, 20, 50, *m*/*m*) and the corresponding sensors upon exposure to PA vapor for 10 s or UV irradiation for 1 min. Scale bar: 1 cm. (b) Multicolor encryption based on CPVCM (1 mM) security ink.

When a large amount of PMMA was added to the security ink to segregate the CPVCM molecules and hinder the formation of nanocrystals, the resulting sensor showed much stronger emission. Specifically, initial sensors made from the PMMA-containing security inks were all olive-emissive possibly due to the restriction of molecular motion caused by the polymer chains. The decreased amination capability observed in the PA fumed sensors (Fig. 7a and Supplementary Fig. 23) verified the effective embedment of CPVCM molecules by PMMA. On the contrary, the CPVCM molecules were expected to undergo some sort of molecular motion in PMMA since its structure could not as rigid as that in the crystal state. Coincidently, a dim fluorescence signal was detected in the initial images but blue emission was observed in the irradiated images (Fig. 7a and Supplementary Fig. 23). Hence, PMMA could unilaterally hinder the amination process and promote the photoarrangement of

CPVCM in filter paper. Moreover, a gradual emission color fading appeared when airing the fumed sensor (Supplementary Fig. 24), and reversible change in the emission color was observed via repeated cycling of PA fuming and standing in the air (Supplementary Fig. 25), demonstrating the high value of CPVCM for information storage.

At last, an all-round information encryption system was proposed. Since four colors (red, orange, olive, and blue) could be achieved in the filter paper, the word "TEAM" which contains four letters, was then chosen as the secret data for demonstration. As shown in Fig. 7b, this information encryption system could be divided into four parts: production, decryption, self-protection, and erasure. First, the production contained writing and locally fixing of the letter "M" by UV irradiation (black arrow) to make it double-secured. Second, the decryption was simple but double secured. One came from the specificity of amination, which could effectively reduce random decoding in real applications (red arrow),[49] the other came from the variability of the reading model since the decrypted data contained text with four different colors. It was worth noting that the signal could still be read after standing for 10 min (Supplementary Fig. 26a), which solved the concerns related to reading time. Third, self-protection was achieved due to the spontaneous reversibility of the amination (blue arrow) and could have an extraordinary effect in preventing the leakage of the decrypted data. At last, the erasure was realized through the irreversible photoarrangement (orange arrow). Since the UV irradiation showed a higher priority than PA fuming in regulating the discoloration of CPVCM, the written letter, the locally fixed letter, and

the decrypted letter could all be erased quickly to result in the globally fixed letter (Fig. 7b and Supplementary Fig. 26b). Besides, the globally fixed letter was inert to PA fuming (Supplementary Fig. 27), which made this erasure process traceless and easy-operation. To sum up, this information encryption system could not only store information in various ways but also prevent information leakage during the whole process, demonstrating the high value of this all-round information encryption system.

Conclusion

In summary, we designed and synthesized a novel multiresponsive and controllable AIEgen called CPVCM, which could undergo amination and photoarrangement at the same position. The amination with primary amines was fast, highly specific, and spontaneously reversible to produce dramatic discoloration under both daylight and UV illumination. The experimental results revealed the important role of nucleophilicity, steric hindrance, and hydrogen-bond stabilization in the high selectivity of CPVCM toward primary amines. In addition, the photoarrangement was fast and irreversible, and caused emission blue-shift and enhancement. The reaction mechanism was verified by dynamic NMR analysis and theoretical calculations. CPVCM was multiresponsive and capable of undergoing spontaneously reversible amination. Thus, dip-coated films were fabricated for developing colored images and dynamic QR codes. A multicolor and all-round information encryption system was also built by utilizing the multi-controllability of CPVCM. To our knowledge, CPVCM was an example of scarcity for intelligent dynamic coloration. It is anticipated that this work not only develops a smart

luminogen with multiple responsive properties and controllability but also provides a strategy to construct information encryption systems based on luminescent materials.

Materials and methods

Apparatus and reagents. ^{1}H NMR (400 MHz) and ^{13}C NMR (100 MHz) spectra were recorded on a Bruker ARX 400 spectrometer using tetramethylsilane as the internal standard. High-resolution mass spectra (HRMS) were recorded on a GCT premier CAB048 mass spectrometer operated in a MALDI-TOF mode. Ultraviolet-visible (UV-vis) spectra were measured on a Milton Roy Spectronic 3000 Array Spectrophotometer. Fluorescence spectra were measured on an Edinburgh FS5 spectrofluorometer. Single crystal data was collected on a Bruker Smart APEXII CCD diffractometer using graphite monochromated Cu Kα radiation (λ = 1.54178 Å). Absolute QY was collected using an integrating sphere on a Hamamatsu Quantum Yield Spectrometer C11347 Quantaurus.

All the chemicals were used as received without further purification unless otherwise specified. All the chemicals were purchased from Sigma-Aldrich Corp. and J&K Chemical Ltd. All the solvents were purchased from VWR Chemicals Corp. Anhydrous THF was used for fluorescence property investigation. Deionized water was used throughout this study.

Synthesis of CMVMN: 3-Benzyl-5,5-dimethylcyclohex-2-en-1-one was synthesized according to a previous report.[50]3-benzyl-5,5-dimethylcyclohex-2-en-1-one (1.07 g, 5 mmol), malononitrile (396 mg, 6 mmol), and sodium ethoxide (340 mg, 10 mmol) were

dissolved in 30 mL ethanol, and the mixture was heated to 50 °C for overnight reaction. Then it was cooled, concentrated and purified by silica gel chromatography (4:1 hexane/EA) to afford compound PCM as a light-yellow liquid (Yield: 1.08 g, 83%). PCM was well characterized by ^{1}H NMR, ^{13}C NMR, and mass spectroscopy (Supplementary Fig. 2-4). ^{1}H NMR (400 MHz, $CDCl_3$), δ (ppm): 7.35-7.27 (m, 3H), 7.15-7.13 (d, J = 8.0 Hz, 2H), 6.69 (s, 1H), 3.56 (s, 2H), 2.51 (s, 2H), 2.09 (s, 2H), 0.93 (s, 6H). ^{13}C NMR (100 MHz, $CDCl_3$), δ (ppm): 170.4, 161.5, 136.5, 129.1, 129.0, 127.4, 121.1, 113.2, 112.4, 79.5, 45.4, 43.6, 43.0, 32.5, 27.8. HRMS (ESI): calcd. for $C_{18}H_{18}N_2$ $[M-H]^-$: 261.1386; found: 261.1397.

Compound PCM (524 mg, 2 mmol) and 4-oxo-4H-chromene-3-carbaldehyde (418 mg, 2.4 mmol) was dissolved in pyridine (2 mL) under nitrogen, and the mixture was refluxed for 2 h. Then it was cooled, concentrated and purified by silica gel chromatography (1:3 hexane/DCM) to afford CPVCM as a light-yellow solid (Yield: 568 mg, 68%). CPVCN was characterized by ^{1}H NMR, ^{13}C NMR, and mass spectroscopy (HRMS) (Supplementary Fig. 5-7). The single crystal of CMVMN was grown and collected by slow evaporation of a mixed solvent of $CHCl_3$ and EtOAc at room temperature and the detailed data were summarized in Supplementary Table 1. ^{1}H NMR (400 MHz, $CDCl_3$), δ (ppm): 8.25-8.23 (d, J = 8.0 Hz, 1H), 7.67-7.63 (m, 1H), 7.51-7.40 (m, 5H), 7.34-7.32 (d, J = 8.0 Hz, 1H), 7.15-7.14 (d, J = 4.0 Hz, 2H), 7.10 (s, 1H), 6.44 (s, 1H), 2.65 (s, 2H), 2.58 (s, 2H), 1.10 (s, 6H). ^{13}C NMR (100 MHz, $CDCl_3$), δ (ppm): 176.6, 169.4, 156.4, 156.2, 155.6, 142.6, 137.4, 134.1, 130.0, 129.2, 128.9, 126.3, 125.8, 123.8, 123.6, 120.5, 118.2, 113.4, 112.1, 80.3, 42.9, 40.7, 32.5, 28.2.

HRMS (ESI): calcd. for $C_{28}H_{22}N_2O_2$ $[M-H]^-$: 417.1598; found: 417.1607.

CPVCM (83.6 mg, 0.2 mmol) was dissolved in chloroform (10 mL) and stirred under a high-pressure mercury lamp (500 W) for 2 h. Then it was cooled, concentrated and purified by silica gel chromatography (9:1 hexane/EA) to afford HBNCM as a colorless solid (Yield: 71 mg, 85%). HBNCM was well characterized by ^{1}H NMR, ^{13}C NMR, and mass spectroscopy (Supplementary Fig. 14-16). ^{1}H NMR (400 MHz, $CDCl_3$), δ (ppm): 11.91 (s, 1H), 8.19 (s, 1H), 8.02-8.01 (d, J = 4.0 Hz, 1H), 7.92-7.90 (d, J = 8.0 Hz, 1H), 7.71-7.62 (m, 4H), 7.59-7.55 (m, 1H), 7.14-7.12 (d, J = 8.0 Hz, 1H), 7.02 (s, 1H), 6.96-6.92 (t, J = 8.0 Hz, 1H), 2.77 (s, 2H), 2.72 (s, 2H), 1.22 (s, 6H). ^{13}C NMR (100 MHz, $CDCl_3$), δ (ppm): 200.7, 168.9, 163.4, 157.7, 139.5, 136.8, 134.5, 133.5, 132.7, 131.7, 130.3, 129.4, 127.7, 124.7, 124.2, 119.3, 119.1, 118.8, 112.9, 112.1, 81.6, 46.3, 42.9, 33.0, 28.0. HRMS (ESI): calcd. for $C_{28}H_{22}N_2O_2$ $[M+Na]^+$: 441.1573; found: 441.1573.

Spin-coating procedure: A stock solution (10.0 mM) of CMVMN was prepared in DCM. At room temperature, 20 μL of the stock solution was placed on the quartz sheet, which was rotated to spread the fluid by centrifugal force.

General Procedure for Detection: In a test tube, 3 mL of THF (pH 9.0) and 40 μL of 1.0 mM CMVMN were mixed, followed by the addition of an analyte. The final volume was adjusted to 4 mL with THF. After incubation at room temperature for 10 min, the reaction solution was transferred to a quartz cell of 1 cm optical length to measure the absorbance or fluorescence.

Computational details: All structures were optimized using M06-2X functional and

6-31g(d,p) basis set for all atoms. Analytical frequency calculations were carried out at the same level of theory to identify all stationary points as either intermediate (no imaginary frequency) or transition state (only one imaginary frequency) to provide thermal corrections to the free energy. To refine the calculated energy, single-point calculations with a larger basis set of 6-311++g(d,p) were done based on the optimized structures. The solvent effect was included implicitly in the single-point calculations using the SMD continuum solvation model with chloroform as the solvent. The reported free energies in this work were calculated based on the electronic energy from single-point calculations and the Gibbs free energy thermal correction obtained from the vibrational analysis. All calculations were performed with Gaussian 16 program.

References

1 Cuthill, I. C. et al. The biology of color. *Science* **357**, eaan0221 (2017).

2 Cuthill, I. C., Stevens, M., Sheppard, J., Maddocks, T., Párraga, C. A., Troscianko, T. S., Disruptive coloration and background pattern matching. *Nature* **434**, 72–74 (2005).

3 Orteu, A., Jiggins, C.D. The genomics of coloration provides insights into adaptive evolution. *Nat. Rev. Genet.* **21**, 461–475 (2020).

4 Stevens M., Merilaita S. Animal camouflage: Current issues and new perspectives. *Philos. Trans. R. Soc. B Biol. Sci.* **364**, 423–427 (2009).

5 Postema, E. G., Lippey, M. K., Armstrong-Ingram, T. Color under pressure: how multiple factors shape defensive coloration. *Behavioral Ecology* arac056, (2022).

6 How, M. J., Santon, M. Cuttlefish camouflage: blending in by matching

background features. *Current Biology*, **32**, 523–525 (2022).

7 Teyssier, J., Saenko, S. V., Marel D., Milinkovitch, M. C. Photonic crystals cause active colour change in chameleons. *Nat. Commun.* **6**, 6368 (2015).

8 Whiting, M. J. et al. Invasive chameleons released from predation display more conspicuous colors. *Sci. Adv.* **8**, eabn2415 (2022).

9 Ligon, R. A., McGraw, K. J. Chameleons communicate with complex colour changes during contests: different body regions convey different information. *Biol. Lett.* **9**, 20130892 (2013).

10 O'Hanlon J.C., Holwell G.I., Herberstein M.E. Pollinator deception in the orchid mantis. *Am. Nat.* **183**, 126–132 (2014).

11 Sun, L., Zhou, T., Wan, Q.-H., Fang, S.-G. Transcriptome comparison reveals key components of nuptial plumage coloration in crested ibis. *Biomolecules* **10**, 905 (2020).

12 Kim, H., Choi, J., Kim, K.K., Won. P., Hong, S., Ko, S. H. Biomimetic chameleon soft robot with artificial crypsis and disruptive coloration skin. *Nat. Commun.* **12**, 4658 (2021).

13 Wei, S., Li, Z., Lu, W., Liu, H., Zhang, J., Chen, T., Tang, B. Z. Multicolor fluorescent polymeric hydrogels. *Angew. Chem. Int. Ed.* **60**, 8608–8624 (2021).

14 Zhang, X., Chen, L., Lim, K. H., Gonuguntla, S., Lim, K. W., Pranantyo, D., Yong, W. P., Yam, W. J. T., Low, Z., Teo, W. J., Nien, H. P., Loh, Q. W., Soh, S. The pathway to intelligence: using stimuli-responsive materials as building blocks for constructing smart and functional systems. *Adv. Mater.* **31**, 1804540 (2019).

15 Zhang, J., He, B., Hu, Y., Alam, P., Zhang, H., Lam, J. W. Y., Tang, B. Z. Stimuli-responsive AIEgens. *Adv. Mater.* **33**, 2008071 (2021).

16 Chen, W., Pan, Y., Chen, J., Ye, F., Liu, S. H., Yin, J. Stimuli-responsive organic chromic materials with near-infrared emission. *Chin. Chem. Lett.* **29**, 1429–1435 (2018).

17 Bai, L., Bose, P., Gao, Q., Li, Y., Ganguly, R., Zhao, Y. Halogen-assisted piezochromic supramolecular sssemblies for versatile haptic memory. *J. Am. Chem. Soc.* **139**, 436–441 (2017).

18 Xu, B., He, J., Mu, Y., Zhu, Q., Wu, S., Wang, Y., Zhang, Y., Jin, C., Lo, C., Chi, Z., Lien, A., Liu, S., Xu, J. Very bright mechanoluminescence and remarkable mechanochromism using a tetraphenylethene derivative with aggregation-induced emission. *Chem. Sci.* **6**, 3236–3241 (2015).

19 Jia, R., Tian, W., Bai, H., Zhang, J., Wang, S., Zhang, J. Amine-responsive cellulose-based ratiometric fluorescent materials for real-time and visual detection of shrimp and crab freshness. *Nat. Commun.* **10**, 795 (2019).

20 Zuo, M., Qian, W., Li, T., Hu, X.-Y., Jiang, J., Wang, L. Full-color tunable fluorescent and chemiluminescent supramolecular nanoparticles for anti-counterfeiting inks. *ACS Appl. Mater. Interfaces* **10**, 39214–39221(2018).

21 Zhang, H., Li, Q., Yang, Y., Ji, X., Sessler J. L. Unlocking chemically encrypted information using three types of external stimuli *J. Am. Chem. Soc.* **143**, 18635–18642 (2021).

22 Jiang, J., Zhang, P., Liu, L., Li, Y., Zhang, Y., Wu, T., Xie, H., Zhang, C., Cui, J.,

Chen, J. Dual photochromics-contained photoswitchable multistate fluorescent polymers for advanced optical data storage, encryption, and photowritable pattern. *Chem. Eng. J.* **425**, 131557 (2021).

23 Du, J.; Sheng, L.; Xu, Y.; Chen, Q.; Gu, C.; Li, M.; Zhang, S. X. Printable off-on thermoswitchable fluorescent materials for programmable thermally controlled full-color displays and multiple encryption. *Adv. Mater.* **33**, 2008055 (2021).

24 Zhang, Q., Yang, L., Han, Y., Wang, Z., Li, H., Sun, S., Xu, Y. A pH-sensitive ESIPT molecule with aggregation-induced emission and tunable solid-state fluorescence multicolor for anti-counterfeiting and food freshness detection *Chem. Eng. J.* **428**, 130986 (2022).

25 He, J., Yang, Y., Li, Y., He, Z., Chen, Y., Wang, Z., Zhao, H., Jiang, G. Multiple anti-counterfeiting guarantees from simple spiropyran derivatives with solid photochromism and mechanochromism. *Cell Reports Physical Science* **2**, 100643 (2021).

26 Huang, G., Chang, X., Jiang, Y., Lin, B., Li, B. S., Tang, B. Z. Multi-stimuli responsive cyanostilbene derivatives: pH, amine vapor sensing and mechanoluminescence. *Mater. Chem. Front.* **4**, 1720–1728 (2020).

27 Luo, W., Wu, B., Xu, X., Han, X., Hu, J., Wang, G. A triple pH-responsive AIEgen: Synthesis, optical properties and applications. *Chem. Eng. J.* **431**, 133717 (2022).

28 Khazi, M. I., Jeong, W., Kim, J.-M. Functional materials and systems for rewritable paper. *Adv. Mater.* **30**, 1705310 (2018).

29 Zhang, J., Zou, Q. Tian, H. Photochromic materials: more than meets the eye. *Adv.*

Mater. **25**, 378–399 (2013).

30 Liu, S., Liu, X., Yuan, J., Bao, J. Multidimensional information encryption and storage: When the input is light. *Research* **2021**, 7897849 (2021).

31 Luo, W., Wang, G. Photo-responsive Fluorescent Materials with Aggregation-Induced Emission Characteristics. *Adv. Optical Mater.* **8**, 2001362 (2020).

32 Hariharan, P. S., Mothi, E. M., Moon, D., Anthony, S. P. Halochromic isoquinoline with mechanochromic triphenylamine: smart fluorescent material for rewritable and self-Erasable fluorescent platform. *ACS Appl. Mater. Interfaces* **8**, 33034–33042 (2016).

33 Zhang, J., Shen, H., Liu, X., Yang, X., Broman, S. L., Wang, H., Li, Q., Lam, J. W. Y., Zhang, H., Cacciarini, M., Nielsen, M. B., Tang, B. Z. A dihydroazulene-based photofluorochromic AIE system for rewritable 4D information encryption. *Angew. Chem.Int. Ed.* e202208460 (2022).

34 Luo, J., Xie, Z., Lam, J. W. Y., Cheng, L., Chen, H., Qiu, C., Kwok, H. S., Zhan, X., Liu, Y., Zhu, D., Tang, B. Z. Aggregation-induced emission of 1-methyl-1,2,3,4,5-pentaphenylsilole. *Chem. Commun.* **18**, 1740–1741 (2001).

35 Liang, J., Tang, B. Z., Liu, B. Specific light-up bioprobes based on AIEgen conjugates. *Chem. Soc. Rev.* **44**, 2798–2811 (2015).

36 Li, H., Kim, H., Han, J., Nguyen, V., Peng, X., Yoon, J. Activity-based smart AIEgens for detection, bioimaging, and therapeutics: Recent progress and outlook. *Aggregate* **2**, e51 (2021).

37 He, X., Xie, H., Hu, L., Liu, P., Xu, C., He, W., Du, W., Zhang, S., Xing, H., Liu,

X., Park, H., Cheung, T. S., Li, M.-H., Kwok, R. T. K., Lam, J. W. Y., Lu, J., Tang, B. Z. A versatile AIE fluorogen with selective reactivity to primary amines for monitoring amination, protein labeling, and mitochondrial staining. *Aggregate* e239 (2022).

38 Fan, J., Wang, T., Li, C., Wang, R., Lei, X., Liang, Y., Zhang, Z. Synthesis of Benzoaryl-5-yl(2-hydroxyphenyl)methanones via Photoinduced Rearrangement of (E)-3-Arylvinyl-4H-chromen-4-ones. *Org. Lett.* **19**, 5984–5987 (2017).

39 Yang, J., Fang, M., Li, Z. Organic luminescent materials: The concentration on aggregates from aggregation-induced emission. *Aggregate* **1**, 6–18 (2020).

40 Liu, Z., Wang, Q., Zhu, Z., Liu, M., Zhao, X., Zhu, W. H. AIE-based nanoaggregate tracker: high-fidelity visualization of lysosomal movement and drug-escaping processes. *Chem. Sci.* **11**, 12755–12763 (2020).

41 Wang, Z., Wang, T., Zhang, C., Humphrey, M. G. Efficient crystallization-induced emission in fluorenyl-tethered carboranes. Phys. *Chem. Chem. Phys.* **19**, 12928–12935 (2017).

42 Yamaguchi, M., Ito, S., Hirose, A., Tanaka, K., Chujo, Y. Control of aggregation-induced emission versus fluorescence aggregation-caused quenching by bond existence at a single site in boron pyridinoiminate complexes. *Mater. Chem. Front.* **1**, 1573–1579 (2017).

43 Tu. Y., Liu, J., Zhang, H., Peng, Q., Lam, J. W. Y., Tang, B. Z. Restriction of access to the dark state: A new mechanistic model for heteroatom-containing AIE systems. *Angew. Chem. Int. Ed.* 58, 14911–14914 (2019).

44 Zhang, J., Alam, P., Zhang, S., Shen, H., Hu, L., Sung, H. H. Y., Williams, I. D., Sun, J., Lam, J. W. Y., Zhang, H., Tang, B. Z. Secondary through-space interactions facilitated single-molecule white-light emission from clusteroluminogens. *Nat. Commun.* **13**, 3492 (2022).

45 Zhang, H., Tang, B. Z. Through-space interactions in clusteroluminescence. *JACS Au* **1**, 1805−1814 (2021).

46 Yang, S.-Y., Qu, Y.-K., Liao, L.-S., Jiang, Z.-Q., Lee, S.-T. Research progress of intramolecular π-stacked small molecules for device applications. *Adv. Mater.* **34**, 2104125 (2022).

47 Hesske, H., Gloe, K. Hydration behavior of alkyl amines and their corresponding protonated forms. 1. Ammonia and methylamine. *J. Phys. Chem. A* **111**, 9848–9853 (2007).

48 V. A. Zagorevskii, É. K. Orlova, I. D. Tsvetkova, V. G. Vinokurov, V. S. Troitskaya, S. G. Rozenberg, Studies of pyrans and related compounds. *Chem. Heterocycl. Compd.* **7**, 675–680 (1971).

49 Zhou, Q., Qiu, X., Su, X., Liu, Q., Wen, Y., Xu, M., Li, F. Light-responsive luminescent materials for information encryption against burst force attack. *Small* **17**, 2100377 (2021).

50 Terao, Y., Satoh, T., Miura, M., Nomura, M. Regioselective arylation on the γ-position of α,β-unsaturated carbonyl compounds with aryl bromides by palladium catalysis. *Tetrahedron Lett.* **39**, 6203-6206 (1989).

Acknowledgements

We are grateful for financial support from the National Natural Science Foundation of China (21788102), the Research Grants Council of Hong Kong (16307020 and C6014-20W), the Innovation and Technology Commission (ITC-CNERC14SC01), and the Natural Science Foundation of Guangdong Province (201913121205002).